Marine Geology 446 (2022) 106774

Contents lists available at ScienceDirect

Marine Geology

journal homepage: www.elsevier.com/locate/margo

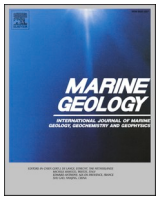

Trace fossil characterization during Termination V and MIS 11 at the western Mediterranean: Connection between surface conditions and deep environment

Alba González-Lanchas [a,*], Javier Dorador [b], Francisco J. Rodríguez-Tovar [b], Francisco J. Sierro [a], José-Abel Flores [a]

[a] Departamento de Geología, Universidad de Salamanca, 37008 Salamanca, Spain
[b] Departamento de Estratigrafía y Paleontología, Universidad de Granada, 18002 Granada, Spain

ARTICLE INFO

Editor: Michele Rebesco

Keywords:
Trace fossils
Primary productivity
Deep oxygenation
Nannofossils
Western Mediterranean
Marine Isotope Stage 11

ABSTRACT

Trace fossil assemblages are studied at Ocean Discovery Program (ODP) Site 977 to characterize the response of the macrobenthic trace maker community to deep paleoenvironmental conditions during the Termination V (TV) and interglacial Marine Isotope Stage (MIS) 11 at the western Mediterranean Alboran Sea. An assemblage composed of *Chondrites*, *Planolites*, *Scolicia*, *Thalassinoides* and *Zoophycos* is identified, showing notable variations in ichnodiversity, abundance and Bioturbation Index, that were analyzed in detail. The integration of ichnological information with sediment color and high-resolution coccolithophore records from Site 977, evidenced that variations in macrobenthic trace maker community are primarily controlled by oxygen availability and surface organic productivity patterns. During TV, high surface organic productivity by intense *Alboran Upwelling System* enhanced the deep organic accumulation that, together with reduced deep-water removal, resulted in a decrease of bioturbation and the formation of an Organic Rich Layer. Moderate and stable surface production through MIS 11c reduced deep food availability, resulting in an oligotrophic and stable deep environment. This is reflected by relatively abundant trace fossils in lighter sediments. Intra-interglacial increase in surface organic production at ~405 ka is evidenced by increased organic matter preservation. Minor impact of western Mediterranean circulation on deep-water removal, but a plausible stronger control by Bernoulli aspiration intensities in the region, is, in overall, observed during these intervals. During the Heinrich-*type* (Ht) events 3 and 2, increased trace fossil diversity and ameliorated oxygenation is driven by limited surface organic production, but intense western Mediterranean deep-water circulation and enhanced regional deep-water removal.

1. Introduction

Changes in deep water oxygen content and organic matter fluxes can lead important impacts on the deep-sea regional environments and macrobenthic trace maker communities (e.g., Wetzel, 1991; Rodríguez-Tovar et al., 2019). In the western Mediterranean - Alboran Sea region, these changes are mainly dependent on the balance between i) bottom-water ventilation, which supplies dissolved oxygen to the seafloor ii) surface ocean productivity, controlling the organic matter fluxes that reach the seafloor and, complementary, iii) terrestrial input and eventual lateral advection of organic particles (see Pérez-Asensio et al., 2020 and references therein).

Bottom ventilation and deep-water removal in the Alboran Sea are controlled by two mechanisms. The first one is the deep-water injection, lifting the preexisting deep-water masses in the region; this mechanism entirely depends on the rates of Western Mediterranean Deep-Water (WMDW) formation at the Gulf of Lion (Fig. 1). The second one is the Bernoulli aspiration of water from below the sill depth (i.e., the depth of the Strait of Gibraltar), that depends on the velocity of the outflow and the density gradient (Fig. 1). Both processes can act independently or in combination, indiscriminately (see Rohling et al., 2015 and references therein). Particularly, calculations accounting for Bernoulli aspiration, shows the capability of this mechanism itself to remove the deep waters from the entire western Mediterranean at the current outflow velocities, this is, solely controlled by the density gradient of water masses existing below the sill depth (Stommel et al., 1973; Rohling et al., 2015).

* Corresponding author.
E-mail address: lanchas@usal.es (A. González-Lanchas).

https://doi.org/10.1016/j.margeo.2022.106774
Received 1 September 2021; Received in revised form 8 March 2022; Accepted 11 March 2022
Available online 16 March 2022

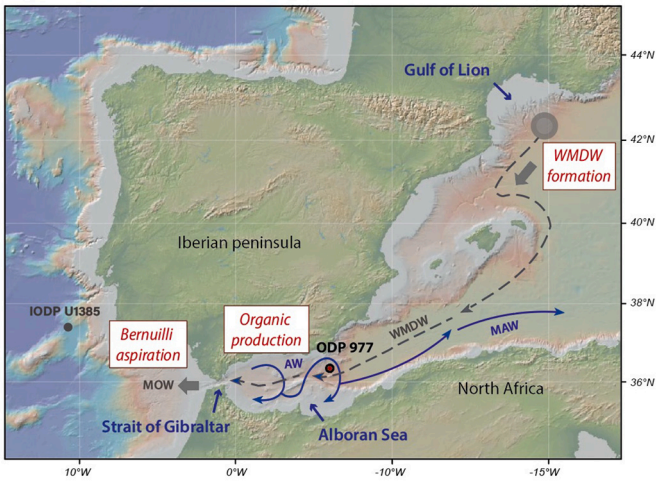

Fig. 1. Location of the Site ODP 977 (red dot) and the main surface and deep currents (respectively, blue, and gray lines and arrows) at the region. Three main mechanisms responsible for production of organic matter at the Alboran Sea (*Organic production*) and the oxygenation bottom waters (*Western Mediterranean Deep Water* – WMDW – *formation* and *Bernoulli aspiration* at the Strait of Gibraltar) are shown. AW: Atlantic Waters, MAW: Modified Atlantic Waters, MOW: Mediterranean Outflow Water. Map source http://www.geomapapp.org/. (For interpretation of the references to color in this figure legend, the reader is referred to the web version of this article.)

Surface phytoplankton primary productivity in the Alboran Sea is mainly controlled by the operation of the *Alboran Upwelling System*, in which the estimation and reconstruction of coccolithophore phytoplankton group production is representative of its intensity and behavior (Fig. 1; see discussion in González-Lanchas et al., 2020). The regional changes in primary productivity evidenced a close relationship with North Atlantic climate evolution via atmospherical connection, from Holocene to older intervals during the Pleistocene (e.g. Ausín et al., 2015; Bazzicalupo et al., 2018, 2020; Colmenero-Hidalgo et al., 2004; Marino et al., 2018).

Paleoichnological analysis is revealed as a suitable tool in paleoenvironmental studies, including paleoceanography and paleoclimatology, providing useful information for the interpretation of parameters such as hydrodynamic energy, oxygenation, sedimentation rate or food availability (Buatois and Mángano, 2011; Knaust and Bromley, 2012). Particularly, changes in ichnological features, such as ichnodiversity, abundance of bioturbation, trace fossils size, or ichnofabrics, allow the interpretation of variations in paleoenvironmental conditions related to Quaternary climates at orbital to millennial scales (e.g., Heinrich Events), affecting macrobenthic tracemaker communities (Goñi et al., 2019; Hodell et al., 2017; Rodríguez-Tovar et al., 2015a; Rodríguez-Tovar et al., 2019; Rodríguez-Tovar et al., 2015b; Rodríguez-Tovar et al., 2020b). Regarding the study area, a few studies have already analyzed the ichnological features in Quaternary sediments (e.g. Alonso et al., 2021; Casanova-Arenillas et al., 2021, 2022). Alonso et al. (2021) developed a multidisciplinary study of the last 25 kyr based on the record of cores MONT PC8 and CONT PC8, drilled around 50 and 150 km western from our study area. They identified a trace fossils assemblage composed of *Asterosoma*, *Chondrites*, *Palaeophycus*, *Planolites*, *Scolicia*, *Taenidium*, *Teichichnus*, *Thalassinoides*, *Phycosiphon* and vertical structures. They differentiated some intervals based on the trace fossil distribution and their evolution, which were related with glacial-interglacial stages. Later, Casanova-Arenillas et al. (2021, 2022) studied around the last 130 kyr from cores drilled in the same study area (i.e., ODP Sites 977 and 976), considering ichnology and geochemistry. They identified a trace fossil assemblage composed of *Chondrites*, *Planolites*, *Thalassinoides*, *Scolicia* and *Zoophycos,* whose variation in abundance and occurrence, together with the geochemical proxies, help them to analyse and discuss the Organic Rich Layers deposited in this area over the last glacial cycle.

As case of study, the Marine Isotope Stage (MIS) 11 has traditionally been considered as a long-lasting (~30 kyr) and extremely warm interglacial on the recent Pleistocene history (e.g. Berger and Wefer, 2003; Hodell et al., 2000; PAGES, 2016; Raynaud et al., 2005; Yin and Berger, 2012), when the extreme collapse of high-latitude ice sheets conditioned an eustatic sea-level rise of about 20 m higher than today (Olson and Hearty, 2009; Raymo and Mitrovica, 2012; Reyes et al., 2014; Roberts et al., 2012). Against such stable interglacial conditions, mid-latitude climate-records has increasingly evidenced contrasting climate instabilities from ~406 ka on centennial (e.g. Koutsodendris et al., 2010; Prokopenko et al., 2010; Tye et al., 2016) to millennial timescales (Oliveira et al., 2016; Tzedakis et al., 2009). Suborbital-scale instabilities associated with the southward incursion of waters with an Arctic origin (Oppo et al., 1998) are comparatively well recorded towards the late MIS 11 (~ 395–374 kyr), as Heinrich-*type* (Ht) events at Iberian latitudes (de Abreu et al., 2005; Hodell et al., 2013; Martrat et al., 2007; Palumbo et al., 2013; Rodrigues et al., 2011; Stein et al., 2009; Voelker et al., 2010). In the Alboran Sea, such climate changes have been recognized from high-resolution coccolithophore records and suggested to impact the conditions of WMDW formation and western Mediterranean thermohaline circulation, responsible of differential stimulation of the *Alboran Upwelling System* and regional primary productivity (González-lanchas et al., 2020). Given this preamble and the general intense dynamic behavior of the surface systems and primary production in this region (Bárcena et al., 2004; Hernández-Almeida et al., 2011), it seems consistent to expect such a dynamical response recorded in the deep environmental levels, where trace makers inhabits. Such a question has, however, scarcely been addressed during the Holocene and Last Glacial Maximum (e.g., Pérez-Asensio et al., 2020), but absent for older intervals of the Pleistocene at this region.

The aim of this contribution is the use of ichnological features and sediment color as proxies to infer bottom conditions in the Alboran Sea environment during the Termination V and MIS 11. To solve the limitations traditionally associated with the ichnological research of unconsolidated modern marine deposits in environments where the differences between biogenic structures and host sediment are weak (Dorador et al., 2014a; Dorador and Rodríguez-Tovar, 2015), software development and high resolution image treatment improved the visibility of ichnological features (Casanova-Arenillas et al., 2020; Dorador and Rodríguez-Tovar, 2018) and allowed detailed sediment color analysis (see methods). On this base, ichnological and sediment color information from modern cores have been frequently included in studies involving paleoenvironmental reconstructions, ocean-atmosphere dynamics and sedimentary basin analysis in the last years (e.g. Dorador and Rodríguez-Tovar, 2016; Evangelinos et al., 2020; Hodell et al., 2017; Miguez-Salas et al., 2019; Rodríguez-Tovar et al., 2015a; Rodríguez-Tovar et al., 2015b; Rodríguez-Tovar et al., 2020a; Rodríguez-Tovar and Dorador, 2014).

These data are integrated with production rates and surface environmental characterization by González-Lanchas et al. (2020), providing an opportunity to i) evaluate the relationship of surface organic production and the deep environmental setting and ii) discuss the influence of bottom ventilation and deep-water removal over the macrobenthic community in the Alboran Sea during the studied interval. This novel multi-proxy approach improves the knowledge about important intra-basin processes and allows hypotheses about climate mechanisms affecting the Mediterranean scale and the evolution of its water exchange dynamics with the Atlantic in such a period of contrasted climate conditions.

2. The western Mediterranean Alboran Sea

In terms of water circulation dynamics, the Alboran Sea represents a transitional area between the semi-enclosed Mediterranean Sea and the

adjacent Atlantic Ocean, connected by the narrow and shallow Strait of Gibraltar (Fig. 1; Pistek et al., 1985). The anti-estuarine Mediterranean circulation is intense in this region and characterized by the strong imprint of both the low saline Atlantic waters in surface (Fig. 1; Atlantic Water, AW), and the deep outflow of the highly saline Mediterranean waters (Fig. 1; Mediterranean Outflow Water, MOW) through the Strait of Gibraltar (Pistek et al., 1985).

The conditions for primary productivity in the region largely depend on the dynamics of the *Alboran Upwelling System*, a multi-cell upwelling system stimulated by the combined effects of i) westerly winds blowing over the southern Iberian coast (Fig. 1) and ii) the intensities of surface Atlantic waters entering the region in relation with the western Mediterranean circulation (Fig. 1; see González-Lanchas et al., 2020 for a complete description). High resolution analysis and reconstruction of primary productivity at the Alboran Sea during Termination V and MIS 11 was already analyzed in the previously mentioned study. It presents a model that dominantly relates the evolution towards intensified *Alboran Upwelling System* with climate-driven enhanced western Mediterranean circulation during episodes of reduced westerly influence over the Mediterranean region, coeval with higher aridity, somewhat observed from the late part of the full interglacial stage MIS 11c. On the contrary, enhanced westerly influence and increased Mediterranean humidity leads to lower surface production, potentially due to reduced western Mediterranean circulation and limited stimulation of the *Alboran Upwelling System*; this scenario is identified with the early phase of the full interglacial MIS 11c.

3. Materials and methods

3.1. Sediment core ODP 977

The ODP Site 977 (36° 1.9′ N; 1° 57.3′ W) is located south of the Cabo de Gata, in the eastern sector of the Alboran Sea Basin (Fig. 1), at a water depth of 1984 m.

The materials in this study are comprised between 67.49 and 58.64 corrected meters below sea floor (cmbsf). It corresponds to the cores 8H-5 to −1 and 7H-7 (and -CC) to −6 of the hole 977A and belongs to the lithological Unit I by Comas et al. (1996). The studied sediments are predominantly composed of open marine-hemipelagic nannofossil and calcareous silty clay and clay facies; the background TOC and % CaCO3 range respectively between 0.17 and 0.8 and 43.2 to 57.7 wt% (Comas et al., 1996).

The chronological framework, the identification of oxygen isotope stages/substages and the sedimentation rate calculations are based on the age assignation proposed by González-Lanchas et al. (2020).

3.2. Ichnological analysis

Ichnological research was supported by digital image analysis (Dorador et al., 2014a, 2014b; Dorador and Rodriguez-Tovar, 2014; Dorador and Rodríguez-Tovar, 2018; Rodríguez-Tovar and Dorador, 2015) applied to high-resolution images from the studied cores. The developed method facilitates ichnological analysis on modern cores, improving visualization of ichnological features. Digital image analysis enables the differentiation between trace fossils (i.e., bioturbational sedimentary structures with sharp outlines and a characteristic recurrent geometry) and biodeformational structures (i.e., with no distinct outlines and no recurrent geometry, determining a mottled background), ichnotaxonomy, relative abundance, cross-cutting relationships, and percentage of bioturbation. Ichnotaxonomic identification was approached to the ichnogenus level based on the recognition of ichnotaxobases in cores (Knaust, 2017). Bioturbation was quantified using the Bioturbation Index (BI), which is defined by seven degrees in a scale ranging from 0 (no bioturbation) to 6 (100% bioturbated) (Reineck, 1963; Taylor and Goldring, 1993)

3.3. Sediment color analysis

Color characterization was conducted on ODP 977 core digital images that are available in the OPD virtual repository http://www-odp.tamu.edu. The selected images were previously treated using Adobe Photoshop CC software to highlight color contrast following method described by Dorador et al. (2014a) based on image adjustments modification, but using the same parameters values in all of them to avoid artefacts. Specifically, *levels* were adjusted to 30, 0.45 and 154; *brightness* and *contrast* was 0 and 74 respectively and finally, *vibrance* was slightly modified to +1 and *saturation* to −2. Then, color was characterized obtaining mean pixel values, using the 8-bits scale (i.e., 0–255), from 2.5 cm thick rectangular sections on the treated core images (Dorador and Rodríguez-Tovar, 2016), excluding the uppermost section to avoid errors associated to sediment core record. A more accurate characterization using thinner sections was discarded due to image resolution limitations.

3.4. Calcareous nannofossil-based proxies and sedimentation rates

Calcareous nannofossil analyses were performed on 181 sediment levels spaced 4 to 6 cm from the hole 977A.

For nannofossil-sample preparation, we followed the random settling technique by Flores and Sierro (1997), with which a homogeneous distribution of coccoliths in the samples is achieved from an initially controlled and regular sample amount. Coccolith identification and quantitative analysis were performed with the use of a double polarized-light Nikon Eclipse 80i petrographic microscope at 1000× magnification. Above the number of 400 coccoliths per sample were identified in a variable number of fields of view. A supplementary census count of 10 fields of view was performed to accurately determine the abundance of other taxa represented in samples with a proportion lower than 1%. Identification of coccolithophore species were based in Young et al. (2003) and the guide of coccolithophore biodiversity and taxonomy Nannotax 3 (Young et al., 2021). Nannofossil data are presented as N, the measure of nannofossil concentration per gram of sediment (nannofossil g^{-1}), calculated following the procedure by Flores and Sierro (1997). The Primary Productivity Proxy (PPP = N small *Gephyrocapsa* + *Gephyrocapsa caribbeanica*) is considered an estimation of surface primary productivity used to trace the state of activation of the *Alboran Upwelling System* (see González-Lanchas et al., 2020 for a complete description). We consider the threshold of PPP under and over 20×10^9 nannofossil g^{-1} to respectively identify the intervals with lower and higher surface primary production in the region, related to the state of activation of the *Alboran Upwelling System.*

The specimens from older stratigraphic levels prior to the studied interval are termed “reworked nannofossil”. The presence of these specimens in the studied sediments is considered potentially indicative of depositional processes related to changes in the intensity of deep circulation in the western Mediterranean. These values were obtained in a separate counting in 10 fields of view and expressed as natural logarithm (Ln) of the N reworked (nannofossil g^{-1}).

Sedimentation rates during the studied interval are derived from the adopted age model.

4. Results

4.1. Ichnological assemblage

Trace fossil assemblage through the studied interval mainly consists of *Chondrites*, *Planolites*, *Scolicia*, *Thalassinoides* and *Zoophycos* (Figs. 2 and 3), that can be assigned to the *Zoophycos* ichnofacies, typical of deep-sea environments, below storm-wave base in outer-shelf to slope deposits (Uchman and Wetzel, 2011). In this general context, significant variations in ichnodiversity, relative abundance and degree of bioturbation are observed.

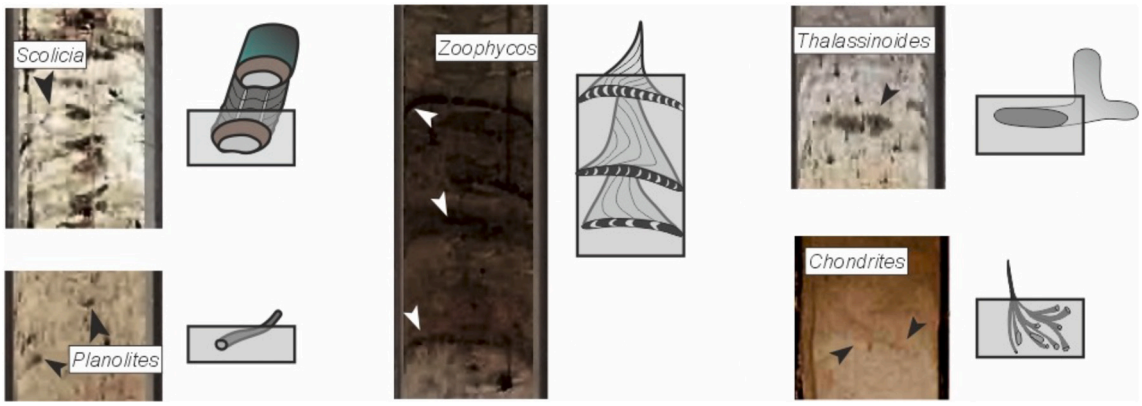

Fig. 2. Core captions and diagrams of the identified trace fossils. Core diameter is around 7 cm for scale.

The TV reveals an upward change in trace fossil assemblage and color, from cm 80 to cm 0 in core 8H-5. From cm 80 to around cm 35, frequent discrete traces of *Planolites* and *Thalassinoides* have been observed in light sediments. From that point to the top of the core, Bioturbation Index (BI) and ichnodiversity show a decreasing trend. *Planolites* and *Thalassinoides* are absent and *Zoophycos* is registered as the dominant trace fossil. This is almost exclusive, except on top of the core where light filled *Thalassinoides* are observed. The presence of *Zoophycos* coincides with darker sediments (Figs. 3 and 4c,f).

A significant change in the ichnological features is observed between TV and the beginning of the full interglacial MIS 11c in cores 8H-4, 8H-3 and 8H-2 (Fig. 3), which is also observed in the color analysis (Fig. 3 and Fig. 4c, f). The lower part of MIS 11c, from cm 140 to around cm 90 in core 8H-4, is characterized by a heavily bioturbated sediment, mainly consisting of *Scolicia*. After that, *Scolicia* disappears and a trace fossil assemblage with *Thalassinoides* and *Planolites* characterizes the rest of the full interglacial MIS 11c, from cm 90 in core 8H-4 to top of core 8H-2 (Figs. 3 and 4f).

The late MIS 11 (MIS 11b) shows variations in ichnological features; the beginning of this part of the record, corresponding to cm 50 to 0 of the core 8H-2, shows the same previous pattern with the record of scarce *Thalassinoides* and *Planolites* in darker host sediments (i.e., similar to the full interglacial MIS11c). The rest of the late MIS 11 shows significant changes in the ichnological features and color record, with a similar pattern in the two studied Heinrich *types* (Ht3 and Ht2; Figs. 3 and 4c, f).

At the Ht3 and Ht2, the trace fossil assemblage is relatively abundant, mainly consisting of *Chondrites*, *Planolites*, *Thalassinoides* and *Zoophycos* (Figs. 3 and 4f). The interval between cm 130 to cm 30 of core 8H-1 in Ht3 can be correlated with the entire Ht2, at core 7H-CC and core 7H-7 (Figs. 3 and 4f). In general, a similar upward trend is observed in both Heinrich *types*: a lighter colored lower part, first scarcely bioturbated and then with the presence of *Planolites*, which shows an upward progressive increase in abundance of traces and ichnodiversity with *Chondrites*, *Thalassinoides* and *Zoophycos* associated to darker sediments.

At the MIS 11- MIS 10 transition, corresponding to the entire core 7H-6, it is observed a decrease in BI and ichnodiversity with respect to the previous Ht2, with scarce and disperse *Thalassinoides* and *Planolites*, showing a similar pattern than that recorded at cm 50 to 0 in core 8H-2 at the late MIS 11 (Figs. 3 and 4f).

4.2. Changes in sediment color

Mean pixel color values characterization reveals significant sediment color changes through the studied intervals (Fig. 4c). From the bottom to the top, we can identify the following evolution. The first 40 cm show a medium color characterized by an average pixel value of 125, but it drastically decreases in the uppermost 20 cm of the 8H-5 core, associated to the last part of the TV (Fig. 4c), reaching 10 as the average value.

Then, an abrupt change to lighter sediments, 180 in average, is identified at the beginning of the full interglacial MIS 11c (Fig. 4c). From this point to 406 ka, approximately, the mean pixel value shows a gradual decreasing trend to darker sediments characterized by 70 as average value (Fig. 4c). This trend has some local and short intervals characterized by darker sediments, usually linked to a scarce presence of trace fossils. Finally, the last part of the full interglacial MIS 11c (i.e., approximately from 406 to 396 ka) is represented by light sediments with an average color value of 210 (Fig. 4c).

At MIS 11b, right after the full interglacial MIS 11c, a decreasing trend in color values is observed, reaching minimum values (40 as average) in the Heinrich *type* interval Ht3 (Fig. 4c). An increasing trend is observed until the end of the studied interval, interrupted by a decrease in the mean pixel color values during the Ht2, represented by an average mean pixel value of 60 (Fig. 4c).

4.3. Sedimentation rates

The sedimentation rate at Site 977 changed between 12 and 22 cm kyr^{1} during MIS 12/11 and MIS 11 (Fig. 4a).

The low sedimentation rates during the glacial period were followed by an average sedimentation rate of ~15 cm kyr^{-1} between the onset of MIS 11 (~424 ka) and until the end of the full interglacial MIS 11c (~387 ka). The sedimentation rate increased between 387 and 377 ka in MIS 11b. A final decrease towards an average of ~15 cm kyr^{-1} is recorded at the end of the studied interval, during the MIS 11/10 transition (Fig. 4a).

4.4. Changes in surface primary productivity and nannofossil-derived proxies

The average of the total N and PPP respectively range between 10 and 60 and 8–40 10^{9} nannofossil g^{-1} during the interval (Fig. 4b). Higher PPP, above 20×10^{9} nannofossil g^{-1}, is observed: i) between 428 and 423 ka at the TV; ii) from 406 to 392 ka, at the late phase of the period of full interglacial conditions in MIS 11c, and transition to the late stage of the MIS 11, MIS 11b, and iii) at two intervals with large PPP values between 389 and 386 ka and 383 to 376 ka of MIS 11b (Fig. 4b). Lower PPP, under the mentioned values, are observed: i) at the late phase of TV included in this record, until 428 ka; ii) continuously within the most part of the full interglacial MIS 11c, until 406 ka and iii) during the occurrence of Ht 3 and 2, respectively centered at ~390 and 383 ka (Fig. 4b).

The percentages of reworked nannofossils (expressed as natural logarithm, Ln, reworked), are comparatively higher in two intervals between: i) ~430 to 417 ka at the TV and the early MIS 11c, and ii)

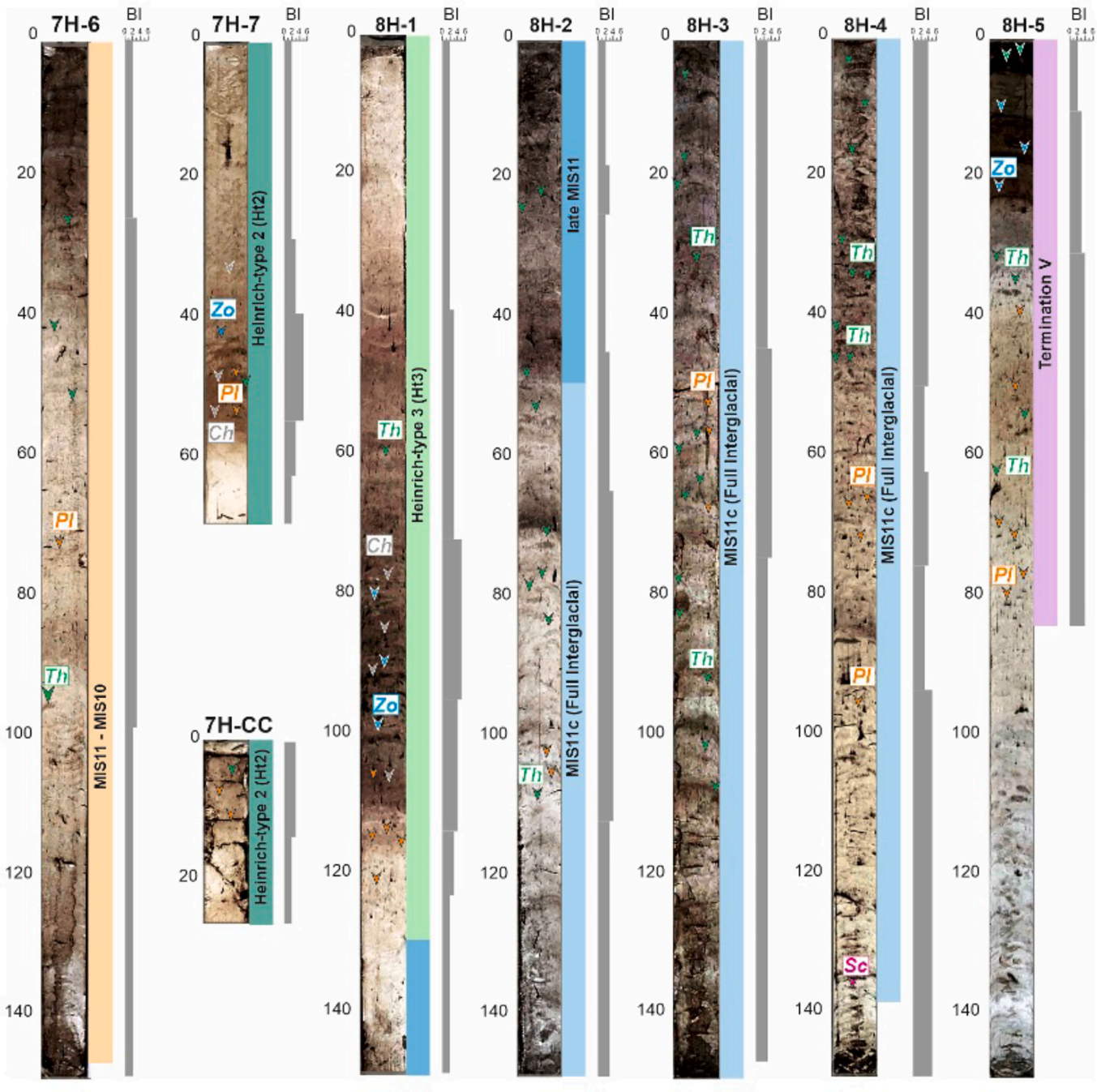

Fig. 3. Schematic representation of the trace fossil assemblage and Bioturbation Index (BI) identified in sediment cores 8H-5 to 7H-6 of Site ODP 977, corresponding to the time interval that includes Termination V and interglacial MIS 11. The limits between isotopic substages and the location of Heinrich *type* (Ht) events 3 and 2 were based on the $\delta^{18}O$ of *Globigerina bulloides* and $U^{K'}_{37}$-SST in González-Lanchas et al. (2020). Trace fossil assemblage *Scolicia* (*Sc*), *Planolites* (*Pl*), *Thalassinoides* (*Th*), *Zoophycos* (*Zo*) and *Chondrites* (*Ch*).

~406 to 396 ka, during the late phase of MIS 11c. Intermediate values with high variability are observed during the rest of the record (Fig. 4f).

5. Discussion

In the following sections we discuss the relationship between conditions of surface organic production, deep oxygenation (i.e., sea-bottom and/or pore water) and live benthic environment. We propose a dynamic model integrating the regional changes in deep-water removal in the Alboran Sea and the intensity of western Mediterranean circulation, driven by climate forcing dynamics.

5.1. Termination V (TV)

The PPP is moderate between 430 and 423 ka at the TV, with an increase centered at ~425 ka. Sedimentation rates increases, as well, in this interval but it does not follow the same pattern as the PPP. Thus, the increased N and PPP between 428 and 422 ka, without a clear connection with the sedimentation rates, lead us to relate them with an increase in surface primary production during the TV (Fig. 4a, b).

The replacement of frequent *Planolites* and *Thalassinoides* during the late MIS 12 (~ 429–425 ka Figs. 3 and 4f) by dominant *Zoophycos* near the onset of the full interglacial MIS 11c (~423 ka; Figs. 3 and 4f),

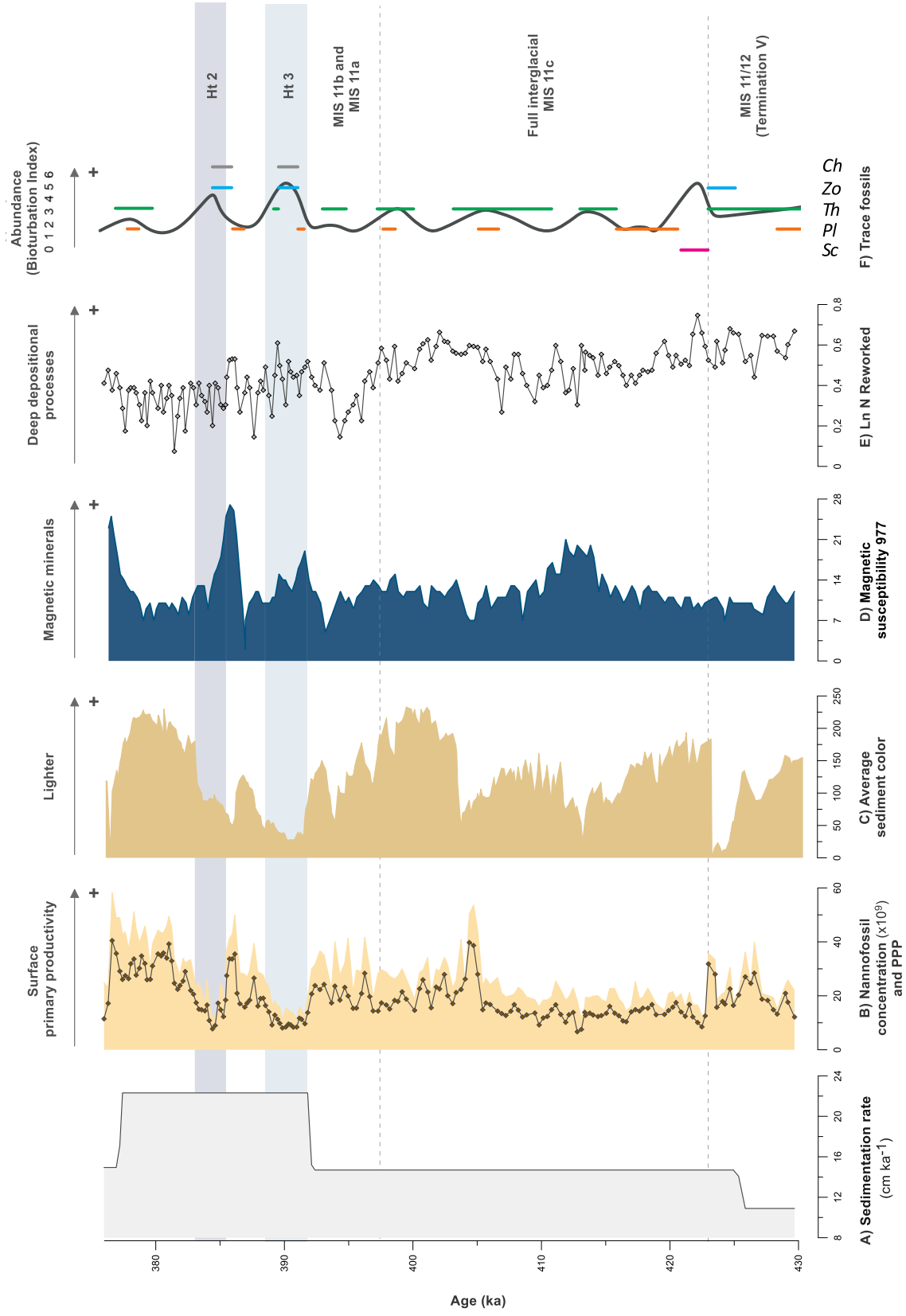

Fig. 4. Integration of ichnological and sedimentological data with the calcareous nannofossil proxies and sedimentation rates during the studied interval. A) Sedimentation rate (cm kyr^{-1}) calculated based on age model by González-Lanchas et al. (2020); B) Total amount of calcareous nannofossil in sediments (Total N) and Primary Productivity Proxy (PPP; nannofossil $g^{-1} \times 10^9$); C) Sediment color profile (average pixel color); D) Magnetic susceptibility at Site 977 (Comas et al., 1996); E) Percentages of reworked nannofossil; F) Trace fossil assemblage; *Scolicia* (*Sc*), *Planolites* (*Pl*), *Thalassinoides* (*Th*), *Zoophycos* (*Zo*) and *Chondrites* (*Ch*) and their abundance represented by the Bioturbation Index (gray curve).

together with a decrease in bioturbation abundance and ichnodiversity and a color shift from lighter to darker sediments, indicate an abrupt change in bottom water properties at the end of TV (Fig. 4c and f). The enhanced surface production through this interval (Fig. 4b) would have generated a progressive increase in the organic matter supply to the deep environment, leading to comparatively high food availability for the macrobenthic communities, which resulted in an eutrophic benthic habitat (Fig. 4f), as revealed by the presence of *Zoophycos* in dark color sediments (Rodríguez-Tovar et al., 2015b). *Zoophycos* is a deep tier structure produced by vermiform animals (Löwemark, 2015), whose presence in Quaternary materials has been related, in particular, to glacial periods of intensive seasonal productivity and high organic carbon fluxes under intermediate sedimentation rates from 5 to 20 cm ka^{-1} (Dorador et al., 2016; Dorador et al., 2019), and usually when bottom water ventilation is low (Rodríguez-Tovar et al., 2015b).

The increased total organic carbon reaching values of 0.8 wt% at ~424.5 ka (Comas et al., 1996) together with the maxima reduction in average sediment color (Fig. 4c), indicate this must correspond to one of the levels of Organic Rich Layer formation at Site 977 (Casanova-Arenillas et al., 2021, 2022; Murat, 1999). These are typically found during deglacial times in the western Mediterranean (see Rogerson et al., 2008), occurring during the TV in this case. Organic Rich Layers can be formed by higher organic fluxes to the seafloor or by reduced rates of deep-water renewal. The correspondence of this type of organic deposits at Site 977 with periods of only moderate summer insolation, assessed early hypothesis about the important role of local intensifications in upwelling dynamics in strong connection with jet-like Atlantic inflow (von Grafenstein et al., 1999). An intensification of the *Alboran Upwelling System* between ~430 and 423 ka at TV (González-Lanchas et al., 2020), observed in the PPP increase (Fig. 4b), points to the role of primary productivity in the formation of the ORL. However, if organic carbon flux from the surface were the only cause of bottom reduction in oxygenation, an increase of higher magnitude in the carbon supply out of the mixed layer than that recorded in the PPP (Fig. 4b) would be required (see Bethoux and Gentili, 1999). In agreement with Rodríguez-Tovar et al. (2015a), lowered bottom water ventilation is required, as well, to produce an impoverished benthic environment comparable to that recorded during this interval (Figs. 3 and 4f). Thus, it seems plausible that a lower rate of deep-water renewal of the Western Mediterranean Deep Water in the Alboran Basin would be necessary as a second mechanism involved to produce the reconstructed lower oxygenated bottom waters.

A lower renewal of bottom waters during TV is consistent with i) lowered rates of WMDW formation in the Gulf of Lion and/or ii) decreased aspiration at the Strait of Gibraltar (Rohling et al., 2015). An intensification of the *Alboran Upwelling System* between ~430 and 423 ka entails an enhanced western Mediterranean circulation during the TV by overall enhancement in WMDW formation (González-Lanchas et al., 2020). As such, we hypothesize about a reduction in the intensities of the Bernoulli aspiration at the Strait of Gibraltar during TV as a plausible mechanism to reduce the regional deep-water removal. This process, together with the enhanced local surface production, seems to plausibility explain the recorded lowered deep oxygenation setting, at least at the level where the macrobenthic community inhabits and ORL deposition (Figs. 3 and 4).

5.2. Full interglacial MIS 11c

The PPP profile is almost constant, with moderate values between 423 and 405 ka, from when a sudden increase is observed, leading to slightly higher values until 392 ka, after the end of the full interglacial MIS 11c, at MIS 11b (Fig. 4b). Intermediate sedimentation rates are constant for the complete interval, so the intra-interglacial N and PPP variability is interpreted as primarily modulated by an increase in surface primary production (Fig. 4a and b).

After the TV, surface primary production abruptly decreases at the onset of MIS 11c and increased bioturbation and abundant traces of *Scolicia* are observed in lighter sediments (Fig. 4b and f). These features represent an important shift in the deep environmental conditions, in which, aside the high amounts of benthic food availability indicated by the presence of *Scolicia* (Kröncke, 2006; Wetzel, 2008), there is a substantial improvement in the oxygenation of deep sedimentary levels compared to TV (Fig. 4f). Rapid burial of the organic matter reaching the bottom, triggered by the slightly increased sedimentation rates after TV (Fig. 4a) together with the reduced rate of surface organic production (Fig. 4b), avoided oxidation at the sea floor, resulting in wide oxygen availability for *Scolicia* trace makers, at least at the level where these organisms inhabit. These conditions in sediments are interpreted as the plausible evidence of amelioration in deep oxygenation in the western Mediterranean, linked to an early increase/restoration in the intensity of the aspiration at the Strait of Gibraltar after its weakening during TV. Such aspiration increase could be responsible for the abrupt redepositional deep processes, as observed by the increased amount of reworked nannofossils in sediments (Fig. 4e).

Following the disappearance of *Scolicia* at ~419 ka, the dominance of *Thalassinoides* and *Planolites* in relatively light-colored sediments is observed as a constant feature, since ~416 ka, during the rest of the full interglacial interval (Fig. 4c). This ichnological pattern indicates a change towards an oligotrophic environment compared to the onset of MIS 11c, but still under relatively well oxygenated conditions. More specifically, the shallow tier habitat indicated by *Planolites* (see Keighley and Pickerill, 1995; Pemberton and Frey, 1982; Rodríguez-Tovar and Uchman, 2004) and the shallow/middle tier *Thalassinoides* inhabiting soft cohesive sediments (see Ekdale, 1992; Ekdale et al., 1984; Fürsich, 1973; Rodríguez-Tovar and Uchman, 2004; Schlirf, 2000), restrict our reconstruction at the uppermost centimeters of the substrate.

In the absence of significant changes in sedimentation rate for the interval, such a limited diversity in the macrobenthic trace maker community seems to be consistent with the reduction of surface organic input due to the reduced interglacial primary production up to 405 ka (Fig. 4b). Thus, the reconstructed relatively high oxygen content in sediments could be the result of low deep oxygen consumption due to the weak supply of organic matter from the surface (Fig. 4b and c). Under relatively steady and oligotrophic deep environmental conditions as such, modest oscillations in surface organic productivity, as recorded up to 405 ka (Fig. 4b), could produce an amplified reduction in the bottom oxygen availability, explaining the recorded interruptions in bioturbation (Figs. 3 and 4f).

The intra interglacial increase in surface primary productivity, from 405 ka upward (Fig. 4b), seems to have had a strong impact on the deep environmental conditions, triggered by a plausible progressive increase in the transference mechanism and accumulation of organic matter to the deep setting, as evidenced by the progression from lighter to darker sediments towards this part of the record (Fig. 4c), together with a coupled decrease in magnetic susceptibility (Fig. 4d). Such intra interglacial change has been considered to be representative of a change in the Iberian interglacial winter climates, changing from higher humidity to more arid conditions (Oliveira et al., 2016). In terms of western Mediterranean circulation, this shift has been proposed to exert the observed impact on surface organic production, from reduced to increased PPP, triggered by an intensification in the *Alboran Upwelling System* at 405 ka (González-Lanchas et al., 2020). Such intra interglacial atmospherical control on coccolithophore communities and surface production is not an isolated fact, but also observed at the nearby Atlantic Site IODP U1385 (González-Lanchas et al., 2021). The increased WMDW formation by more intense, colder winter winds in the Gulf of Lion at this time (González-Lanchas et al., 2020) does not seem, however, to have a clear imprint in the oxygenation of the sediments at the level where the macrobenthic communities inhabit. As such, we suggest that a coeval reduction in the Bernoulli aspiration, reducing deep water removal and favoring the organic accumulation and preservation, should occur associated to the interglacial progress. An imprint of this

mechanism, reducing regional deep re-depositional processes, is supported by the reduction of reworked nannofossils (Fig. 4e) during this interval.

5.3. Heinrich-type (Ht) events 3 and 2

The PPP is minimum during Ht3 (~391 ka) and Ht2 (~385 ka; Fig. 4b). The high sedimentation rates suggest that other non-biogenic material could obscure the surface organic productivity signal, that could be slightly higher than reconstructed from the absolute N and PPP (Fig. 4a and b). This is well evidenced by the increased values of magnetic susceptibility at Ht3 and Ht2 (Fig. 4d).

Trace fossil assemblage during both episodes is relatively abundant and mainly characterized by a similar pattern: lighter colored and scarcely bioturbated sediments are registered at the lower part of the sequences (Fig. 4f). The presence of *Planolites* at the base of the Ht gives rise to a progressive upward increase in the abundance of traces and ichnodiversity, with *Zoophycos*, *Chondrites* and *Thalassinoides* associated to darker sediments towards the central part of Ht3 and Ht2 (Fig. 4f).

Ichnological records at different latitudes in the Atlantic revealed the occurrence of two-phase conditions during Heinrich stadial of the last glacial cycle (Baas et al., 1997; Baas et al., 1998; Rodríguez-Tovar et al., 2019), characterized, in overall, by: i) an early phase of important bottom-water stagnation and highly dysoxic conditions related to Atlantic Meridional Overturning Circulation (AMOC) slowdown, and ii) deep oxygen amelioration in water bodies and re-established biodiversity in the trace maker community shortly after the deposition of the ice-rafted detritus (IRD) layer. As in the case of Heinrich stadial events during the last glacial cycle, the occurrence of both Heinrich-*type* 3 and 2 during the late MIS 11 has been linked to AMOC disruptions from iceberg calving of British ice sheet origin (de Abreu et al., 2005; Rodrigues et al., 2011). Thus, a comparable deep dynamic during the occurrence of Ht is expected to occur in the Atlantic. This has been recently confirmed by the identification of comparable surface hydrological structure of halocline formation and nutrient upward limitation at the IODP Site U1385 during the occurrence of Ht3 and Ht2 (González-Lanchas et al., 2021).

In the western Mediterranean, low primary productivity rates during Ht3 and Ht2 have been primarily related to the impact of the cold surface waters of subpolar origin entering the Strait of Gibraltar over the phytoplankton community at the Alboran Sea (González-Lanchas et al., 2020; Marino et al., 2018). Climatically, semi-arid conditions at the Mediterranean maintaining high rates of WMDW formation and intense *Alboran Upwelling System,* have been proposed during the Ht3 and Ht2 (González-Lanchas et al., 2020). This idea agrees with the relatively light color of the sediments through these episodes at 977 (Fig. 4d) suggesting, indeed, that important changes in the conditions of oxygenation of the deep waters did not play a determining role in the western Mediterranean during Ht events. Rather, a reduction in surface supply of organic matter (Fig. 4c), or the effect of the increased sedimentation rates and accumulation of detrital particles seems to be an important factor promoting a quick burial and the trace fossil scarcity recorded at the beginning of the sequences (Fig. 4f).

The progressive increase in organic matter supply to the deep setting through the upper part of each event Ht3 and Ht2 could be promoted by an improvement in surface conditions for organic production. Potentially less cold-temperature limitation on coccolithophore proliferation (González-Lanchas et al., 2020; Marino et al., 2018) together with a well-oxygenated deep setting, could favour the increase in diversity and abundance of the trace fossil assemblage (Figs. 3 and 4f). However, the dilution effect caused by the increased accumulation of detrital minerals during both intervals (i.e., magnetic minerals recorded in the profile of magnetic susceptibility; Fig. 4d) could have obscured, in some extent, the surface productivity signal (Fig. 4c).

6. Conclusions

Our results evidence a preponderant connection of surface organic production rates with deep organic matter availability and macrobenthic conditions in the Alboran Sea, where the modest changes in sedimentation rate played a secondary role. During Termination V, the high surface organic productivity by intense *Alboran Upwelling System* were transferred to the deep environment, where reduced deep-water removal and poor oxygenation led to preservation of organic matter, resulting in the decrease of macrobenthic activity and the formation of an Organic Rich Layer. During the early full interglacial MIS 11c, improved deep oxygenation is recorded, generating better conditions for macrobenthic tracemakers. This oligotrophic deep environment is the result of moderate and stable surface production and intermediate sedimentation rates. Intra-interglacial increase in surface production increased organic matter availability in the deep environment, which, together with reduced deep-water removal, favored the organic preservation. The impact of the WMDW formation in the Gulf of Lion on the regional benthic environment and the regional deep oxygenation was minor, suggesting its potential minor influence on the regional deep oxygenation at this time and scale. This observation supports the recent growing suggestions about the importance of the density gradient between water masses at the Strait of Gibraltar and the resulting intensities of the Bernoulli aspiration on deep water removal in this region. However, more studies are needed to verify this observation, where integrated surface to deep approaches, as conducted in this study, may serve as a reference. Well oxygenated deep setting and trace fossil diversity during Ht3 and Ht2 supports previous determinations about an intense *Alboran Upwelling System* together with intense western Mediterranean circulation during the occurrence of these extreme episodes.

Data statement

Calcareous nannofossil data used in this study is stored in the public repository PANGAEA® as: González-Lanchas, Alba; Flores, José-Abel; Sierro, Francisco J.; Bárcena, María Ángeles; Cortina, Aleix; Cacho, Isabel; Grimalt, Joan O (2020): Nannofossil, opal phytolith, stable isotopes and $U^{K'}_{37}$ Sea Surface Temperature record from ODP Site 977 during the MIS 11. https://doi.org/10.1594/PANGAEA.921235. Regarding ichnological analysis, all data obtained during this study are summarized in the present article. Anyway, original images and datasets are available by request.

Declaration of Competing Interest

The authors declare that they have no known competing financial interests or personal relationships that could have appeared to influence the work reported in this paper.

Acknowledgments

This study was supported by the predoctoral FPU contract FPU17/03349 awarded to A. González-Lanchas by the Spanish Ministry of Science, Innovation and Universities. The research by JD was funded through the Juan de la Cierva Program (IJC2019-038866-I) by the Spanish Ministry of Science and Innovation. Essential financial infrastructure was provided by the programs RTI2018-099489-B-100 of the Spanish Ministry of Science, Innovation and Universities granted to GGO (Grupo de Geociencias Oceánicas de la Universidad de Salamanca) and CGL2015-66835-P and PID2019-104625RB-100 of the Spanish Ministry of Science, Innovation and Universities and B-RNM-072-UGR18, P18-RT-4074 of the Andalusian Government granted to Ichnology and Palaeoenvironment RG (University of Granada). We thank Alessandra Negri and the two anonymous reviewers, whose comments contributed to improve this manuscript.

References

Alonso, B., Juan, C., Ercilla, G., Cacho, I., López-González, N., Rodríguez-Tovar, F.J., Dorador, J., Francés, G., Casas, D., Vandorpe, T., Vázquez, J.T., 2021. Paleoceanographic and paleoclimatic variability in the Western Mediterranean during the last 25 cal. kyr BP. New insights from contourite drifts. Mar. Geol. 437, 106488.

Ausín, B., Flores, J.-A., Sierro, F.-J., Bárcena, M.-A., Hernández-Almeida, I., Francés, G., Gutiérrez-Arnillas, E., Martrat, B., Grimalt, J.O., Cacho, I., 2015. Coccolithophore productivity and surface water dynamics in the Alboran Sea during the last 25 kyr. Palaeogeogr. Palaeoclimatol. Palaeoecol. 418, 126–140.

Baas, J.H., Mienert, J., Abrantes, F., Prins, M.A., 1997. Late Quaternary sedimentation on the Portuguese continental margin: climate-related processes and products. Palaeogeogr. Palaeoclimatol. Palaeoecol. 130, 1–23.

Baas, J., Schönfeld, J., Zahn, R., 1998. Mid-depth oxygen drawdown during Heinrich events: evidence from benthic foraminiferal community structure, trace-fossil tiering, and benthic δ13C at the Portuguese Margin. Mar. Geol. 152, 25–55.

Bárcena, M.A., Flores, J.A., Sierro, F.J., Pérez-Folgado, M., Fabres, J., Calafat, A., Canals, M., 2004. Planktonic response to main oceanographic changes in the Alboran Sea (Western Mediterranean) as documented in sediment traps and surface sediments. Mar. Micropaleontol. 53 (3–4), 423–445.

Bazzicalupo, P., Maiorano, P., Girone, A., Marino, M., Combourieu-Nebout, N., Incarbona, A., 2018. High-frequency climate fluctuations over the last deglaciation in the Alboran Sea, Western Mediterranean: evidence from calcareous plankton assemblages. Palaeogeogr. Palaeoclimatol. Palaeoecol. 506, 226–241.

Bazzicalupo, P., Maiorano, P., Girone, A., Marino, M., Combourieu-Nebout, N., Pelosi, N., Salgueiro, E., Incarbona, A., 2020. Holocene climate variability of the Western Mediterranean: Surface water dynamics inferred from calcareous plankton assemblages. Holocene 30 (5), 691–708, 0959683619895580.

Berger, W.H., Wefer, G., 2003. On the dynamics of the ice ages: stage-11 paradox, mid-brunhes climate shift, and 100-ky cycle. Geophys. Monogr. Ser. 41–59.

Bethoux, J.P., Gentili, B., 1999. Functioning of the Mediterranean Sea: past and present changes related to freshwater input and climate changes. J. Mar. Syst. 20 (1–4), 33–47.

Buatois, L.A., Mángano, M.G., 2011. Ichnology: Organism-Substrate Interactions in Space and Time. Cambridge University Press.

Casanova-Arenillas, S., Rodríguez-Tovar, F.J., Martínez-Ruiz, F., 2020. Applied ichnology in sedimentary geology: Python scripts as a method to automatize ichnofabric analysis in marine core images. Comput. Geosci. 136, 104407.

Casanova-Arenillas, S., Rodríguez-Tovar, F.J., Martínez-Ruiz, F., 2021. Ichnological analysis as a tool for assessing deep-sea circulation in the westernmost Mediterranean over the last Glacial Cycle. Palaeogeogr. Palaeoclimatol. Palaeoecol. 562, 110082.

Casanova-Arenillas, S., Rodríguez-Tovar, F.J., Martínez-Ruiz, F., 2022. Ichnological evidence for bottom water oxygenation during organic rich layer deposition in the westernmost Mediterranean over the Last Glacial Cycle. Mar. Geol. 443, 106673.

Colmenero-Hidalgo, E., Flores, J.-A., Sierro, F.J., Bárcena, M.A., Löwemark, L., Schönfeld, J., Grimalt, J.O., 2004. Ocean surface water response to short-term climate changes revealed by coccolithophores from the Gulf of Cadiz (NE Atlantic) and Alboran Sea (W Mediterranean). Palaeogeogr. Palaeoclimatol. Palaeoecol. 205, 317–336.

Comas, M., Zahn, R., Klaus, A., 1996. Preliminary results of ODP Leg 161. Proc. Ocean Drill. Program Prelim. Results 161, 1–1679.

de Abreu, L., Abrantes, F.F., Shackleton, N.J., Tzedakis, P.C., McManus, J.F., Oppo, D.W., Hall, M.A., 2005. Ocean climate variability in the eastern North Atlantic during interglacial marine isotope stage 11: a partial analogue to the Holocene? Paleoceanography 20, 1–15.

Dorador, J., Rodriguez-Tovar, F.J., 2014. A novel application of digital image treatment by quantitative pixel analysis to trace fossil research in marine cores. Palaios 29, 533–538.

Dorador, J., Rodríguez-Tovar, F.J., 2015. Application of digital image treatment to the characterization and differentiation of deep-sea ichnofacies. Span. J. Palaeontol. 30, 265–274.

Dorador, J., Rodríguez-Tovar, F.J., 2016. High resolution digital image treatment to color analysis on cores from IODP Expedition 339: approaching lithologic features and bioturbational influence. Mar. Geol. 377, 127–135.

Dorador, J., Rodríguez-Tovar, F.J., 2018. High-resolution image treatment in ichnological core analysis: initial steps, advances and prospects. Earth Sci. Rev. 177, 226–237.

Dorador, J., Rodríguez-Tovar, F.J., Expedition, I., 2014a. Digital image treatment applied to ichnological analysis of marine core sediments. Facies 60, 39–44.

Dorador, J., Rodríguez-Tovar, F.J., Expedition, I., 2014b. Quantitative estimation of bioturbation based on digital image analysis. Mar. Geol. 349, 55–60.

Dorador, J., Wetzel, A., Rodríguez-Tovar, F.J., 2016. Zoophycos in deep-sea sediments indicates high and seasonal primary productivity: Ichnology as a proxy in palaeoceanography during glacial–interglacial variations. Terra Nova 28, 323–328.

Dorador, J., Rodríguez-Tovar, F.J., Mena, A., Francés, G., 2019. Lateral variability of ichnological content in muddy contourites: Weak bottom currents affecting organisms' behavior. Sci. Rep. 9, 1–7.

Ekdale, A., 1992. Muckraking and mudslinging: the joys of deposit-feeding. Short Courses Paleontol. 5, 145–171.

Ekdale, A.A., Bromley, R.G., Pemberton, S.G., 1984. Ichnology: the use of trace fossils in sedimentology and stratigraphy. Soc. Econ. Paleontol. Mineral. 15, 316.

Evangelinos, D., Escutia, C., Etourneau, J., Hoem, F., Bijl, P., Boterblom, W., van de Flierdt, T., Valero, L., Flores, J.-A., Rodriguez-Tovar, F.J., 2020. Late Oligocene-Miocene proto-Antarctic Circumpolar Current dynamics off the Wilkes Land margin, East Antarctica. Glob. Planet. Chang. 191, 103221.

Flores, J., Sierro, F., 1997. Revised technique for calculation of calcareous nannofossil accumulation rates. Micropaleontology 321–324.

Fürsich, F., 1973. A revision of the trace fossils Spongeliomorpha, Ophiomorpha and Thalassinoides. Neues Jb. Geol. Paläontol. Monat. 12, 719–735.

Goñi, M.F.S., Ferretti, P., Polanco-Martínez, J.M., Rodrigues, T., Alonso-García, M., Rodríguez-Tovar, F.J., Dorador, J., Desprat, S., 2019. Pronounced northward shift of the westerlies during MIS 17 leading to the strong 100-kyr ice age cycles. Earth Planet. Sci. Lett. 511, 117–129.

González-Lanchas, A., Flores, J.-A., Sierro, F.J., Bárcena, M.Á., Rigual-Hernández, A.S., Oliveira, D., Azibeiro, L.A., Marino, M., Maiorano, P., Cortina, A., Cacho, I., Grimalt, J.O., 2020. A new perspective of the *Alboran Upwelling System* reconstruction during the Marine Isotope Stage 11: a high-resolution coccolithophore record. Quat. Sci. Rev. 245, 106520.

González-Lanchas, A., Flores, J.A., Sierro, F., Sánchez Goñi, M., Rodrigues, T., Ausin, B., Oliveira, D., Naughton, F., Marino, M., Maiorano, P., Balestra, B., 2021. Control mechanisms of Primary Productivity revealed by calcareous nannoplankton from Marine Isotope Stages 12 to 9 at the Shackleton Site (IODP Site U1385). Paleoceanography and Paleoclimatology 36 (6) e2021PA004246.

Hernández-Almeida, I., Bárcena, M.A., Flores, J.A., Sierro, F.J., Sanchez-Vidal, A., Calafat, A., 2011. Microplankton response to environmental conditions in the Alboran Sea (Western Mediterranean): one year sediment trap record. Mar. Micropaleontol. 78 (1–2), 14–24.

Hodell, D.A., Charles, C.D., Ninnemann, U.S., 2000. Comparison of interglacial stages in the South Atlantic sector of the southern ocean for the past 450 kyr: implifications for Marine Isotope Stage (MIS) 11. Glob. Planet. Chang. 24, 7–26.

Hodell, D., Crowhurst, S., Skinner, L., Tzedakis, P.C., Margari, V., Channell, J.E., Kamenov, G., Maclachlan, S., Rothwell, G., 2013. Response of Iberian Margin sediments to orbital and suborbital forcing over the past 420 ka. Paleoceanography 28, 185–199.

Hodell, D.A., Nicholl, J.A., Bontognali, T.R., Danino, S., Dorador, J., Dowdeswell, J.A., Einsle, J., Kuhlmann, H., Martrat, B., Mleneck-Vautravers, M.J., Rodríguez-Tovar, F. J., Röhl, U., 2017. Anatomy of Heinrich Layer 1 and its role in the last deglaciation. Paleoceanography 32, 284–303.

Keighley, D.G., Pickerill, R.K., 1995. Commentary: The Ichnotaxa Palaeophycus and Planolites: Historical Perspectives and Recommendations.

Knaust, D., 2017. Atlas of Trace Fossils in Well Core: Appearance, Taxonomy and Interpretation. Springer.

Knaust, D., Bromley, R.G., 2012. Trace Fossils as Indicators of Sedimentary Environments. Newnes.

Koutsodendris, A., Müller, U.C., Pross, J., Brauer, A., Kotthoff, U., Lotter, A.F., 2010. Vegetation dynamics and climate variability during the Holsteinian interglacial based on a pollen record from Dethlingen (northern Germany). Quat. Sci. Rev. 29, 3298–3307.

Kröncke, I., 2006. Structure and function of macrofaunal communities influenced by hydrodynamically controlled food availability in the Wadden Sea, the open North Sea, and the deep-sea. A synopsis. Senckenberg. Marit. 36, 123–164.

Löwemark, L., 2015. Testing ethological hypotheses of the trace fossil Zoophycos based on Quaternary material from the Greenland and Norwegian Seas. Palaeogeogr. Palaeoclimatol. Palaeoecol. 425, 1–13.

Marino, M., Girone, A., Maiorano, P., Di Renzo, R., Piscitelli, A., Flores, J.-A., 2018. Calcareous plankton and the mid-Brunhes climate variability in the Alboran Sea (ODP Site 977). Palaeogeogr. Palaeoclimatol. Palaeoecol. 508, 91–106.

Martrat, B., Grimalt, J.O., Shackleton, N.J., de Abreu, L., Hutterli, M.A., Stocker, T.F., 2007. Four climate cycles of recurring deep and surface water destabilizations on the Iberian margin. Science 317, 502–507.

Miguez-Salas, O., Dorador, J., Rodríguez-Tovar, F.J., 2019. Introducing Fiji and ICY image processing techniques in ichnological research as a tool for sedimentary basin analysis. Mar. Geol. 413, 1–9.

Murat, A., 1999. Pliocene-pleistocene occurrence of sapropels in the Western Mediterranean Sea and their relation to Eastern Mediterranean Sapropels. In: Proceedings of the Ocean Drilling Program, Scientific Results, 41, pp. 519–527.

Oliveira, D., Desprat, S., Rodrigues, T., Naughton, F., Hodell, D., Trigo, R., Rufino, M., Lopes, C., Abrantes, F., Goni, M.F.S., 2016. The complexity of millennial-scale variability in southwestern Europe during MIS 11. Quat. Res. 86, 373–387.

Olson, S.L., Hearty, P.J., 2009. A sustained +21m sea-level highstand during MIS 11 (400ka): direct fossil and sedimentary evidence from Bermuda. Quat. Sci. Rev. 28, 271–285.

Oppo, D., McManus, J., Cullen, J., 1998. Abrupt climate events 500,000 to 340,000 years ago: evidence from subpolar North Atlantic sediments. Science 279, 1335–1338.

PAGES, P.I.W.G.o, 2016. Interglacials of the last 800,000 years. Rev. Geophys. 54, 162–219.

Palumbo, E., Flores, J.A., Perugia, C., Emanuele, D., Petrillo, Z., Rodrigues, T., Voelker, A.H., Amore, F.O., 2013. Abrupt variability of the last 24 ka BP recorded by coccolithophore assemblages off the Iberian Margin (core MD03-2699). J. Quat. Sci. 28, 320–328.

Pemberton, S.G., Frey, R.W., 1982. Trace fossil nomenclature and the Planolites-Palaeophycus dilemma. J. Paleontol. 843–881.

Pérez-Asensio, J.N., Frigola, J., Pena, L.D., Sierro, F.J., Reguera, M.I., Rodríguez-Tovar, F.J., Dorador, J., Asioli, A., Kuhlmann, J., Huhn, K., 2020. Changes in western Mediterranean thermohaline circulation in association with a deglacial Organic Rich Layer formation in the Alboran Sea. Quat. Sci. Rev. 228, 106075.

Pistek, P., De Strobel, F., Montanari, C., 1985. Deep-sea circulation in the Alboran Sea. J. Geophys. Res. Oceans 90, 4969–4976.

Prokopenko, A., Bezrukova, E., Khursevich, G., Solotchina, E., Kuzmin, M., Tarasov, P., 2010. Climate in continental interior Asia during the longest interglacial of the past 500 000 years: the new MIS 11 records from Lake Baikal, SE Siberia. Clim. Past 6, 31–48.

Raymo, M.E., Mitrovica, J.X., 2012. Collapse of polar ice sheets during the stage 11 interglacial. Nature 483, 453.

Raynaud, D., Barnola, J.-M., Souchez, R., Lorrain, R., Petit, J.-R., Duval, P., Lipenkov, V. Y., 2005. Palaeoclimatology: the record for marine isotopic stage 11. Nature 436, 39.

Reineck, H.E., 1963. Sedimentgefüge im Bereich der südliche Nordsee. Abh. Senckenb. Naturforsch. Ges. 505, 1–138.

Reyes, A.V., Carlson, A.E., Beard, B.L., Hatfield, R.G., Stoner, J.S., Winsor, K., Welke, B., Ullman, D.J., 2014. South Greenland ice-sheet collapse during marine isotope stage 11. Nature 510, 525.

Roberts, D.L., Karkanas, P., Jacobs, Z., Marean, C.W., Roberts, R.G., 2012. Melting ice sheets 400,000 yr ago raised sea level by 13 m: past analogue for future trends. Earth Planet. Sci. Lett. 357, 226–237.

Rodrigues, T., Voelker, A., Grimalt, J., Abrantes, F., Naughton, F., 2011. Iberian Margin sea surface temperature during MIS 15 to 9 (580–300 ka): Glacial suborbital variability versus interglacial stability. Paleoceanography 26.

Rodríguez-Tovar, F.J., Dorador, J., 2014. Ichnological analysis of Pleistocene sediments from the IODP Site U1385 "Shackleton Site" on the Iberian margin: approaching paleoenvironmental conditions. Palaeogeogr. Palaeoclimatol. Palaeoecol. 409, 24–32.

Rodríguez-Tovar, F.J., Dorador, J., 2015. Ichnofabric characterization in cores: a method of digital image treatment. Ann. Soc. Geol. Pol. 465–471.

Rodríguez-Tovar, F.J., Uchman, A., 2004. Trace fossils after the K–T boundary event from the Agost section, SE Spain. Geol. Mag. 141, 429–440.

Rodríguez-Tovar, F.J., Dorador, J., Grunert, P., Hodell, D., 2015a. Deep-sea trace fossil and benthic foraminiferal assemblages across glacial Terminations 1, 2 and 4 at the "Shackleton Site"(IODP Expedition 339, Site U1385). Glob. Planet. Chang. 133, 359–370.

Rodríguez-Tovar, F.J., Dorador, J., Martin-Garcia, G.M., Sierro, F.J., Flores, J.A., Hodell, D.A., 2015b. Response of macrobenthic and foraminifer communities to changes in deep-sea environmental conditions from Marine Isotope Stage (MIS) 12 to 11 at the "Shackleton Site". Glob. Planet. Chang. 133, 176–187.

Rodríguez-Tovar, F.J., Dorador, J., Hodell, D.A., 2019. Trace fossils evidence of a complex history of nutrient availability and oxygen conditions during Heinrich Event 1. Glob. Planet. Chang. 174, 26–34.

Rodríguez-Tovar, F., Miguez-Salas, O., Dorador, J., 2020a. Image processing techniques to improve characterization of composite ichnofabrics. Ichnos 27, 258–267.

Rodríguez-Tovar, F.J., Dorador, J., Mena, A., Francés, G., 2020b. Regional and global changes during Heinrich Event 1 affecting macrobenthic habitat: ichnological evidence of sea-bottom conditions at the Galicia Interior Basin. Glob. Planet. Chang. 192, 103227.

Rogerson, M., Cacho, I., Jimenez-Espejo, F., Reguera, M., Sierro, F.J., Martinez-Ruiz, F., Frigola, J., Canals, M., 2008. A dynamic explanation for the origin of the western Mediterranean organic-rich layers. Geochem. Geophys. Geosyst. 9.

Rohling, E.J., Marino, G., Grant, K.M., 2015. Mediterranean climate and oceanography, and the periodic development of anoxic events (sapropels). Earth Sci. Rev. 143, 62–97.

Schlirf, M., 2000. Upper Jurassic trace fossils from the Boulonnais (northern France). Geol. Palaeontol. 34, 145–213.

Stein, R., Hefter, J., Grützner, J., Voelker, A., Naafs, B.D.A., 2009. Variability of surface water characteristics and Heinrich-like events in the Pleistocene midlatitude North Atlantic Ocean: Biomarker and XRD records from IODP Site U1313 (MIS 16–9). Paleoceanography 24.

Stommel, H., Bryden, H., Mangelsdorf, P., 1973. Does some of the Mediterranean outflow come from great depth? Pure Appl. Geophys. 105 (1), 879–889.

Taylor, A.M., Goldring, R., 1993. Description and analysis of bioturbation and ichnofabric. J. Geol. Soc. Lond. 150, 141–148.

Tye, G., Sherriff, J., Candy, I., Coxon, P., Palmer, A., McClymont, E., Schreve, D., 2016. The δ18O stratigraphy of the Hoxnian lacustrine sequence at Marks Tey, Essex, UK: implications for the climatic structure of MIS 11 in Britain. J. Quat. Sci. 31, 75–92.

Tzedakis, P., Pälike, H., Roucoux, K., De Abreu, L., 2009. Atmospheric methane, southern European vegetation and low-mid latitude links on orbital and millennial timescales. Earth Planet. Sci. Lett. 277, 307–317.

Uchman, A., Wetzel, A., 2011. Deep-sea ichnology: the relationships between depositional environment and endobenthic organisms. In: Developments in Sedimentology. Elsevier, pp. 517–556.

Voelker, A.H., Rodrigues, T., Billups, K., Oppo, D.W., McManus, J.F., Stein, R., Hefter, J., Grimalt, J.O., 2010. Variations in Mid-Latitude North Atlantic Surface Water Properties during the Mid-Brunhes (MIS 9–14) and their Implications for the Thermohaline Circulation.

von Grafenstein, R., Zahn, R., Tiedemann, R., Murat, A., 1999. Planktonic δ18O records at Sites 976 and 977, Alboran Sea: stratigraphy, forcing, and paleoceanographic implications. In: Zahn, R., Comas, M.C., Klaus, A. (Eds.), Proceedings ODP, Scientific Results. Ocean Drilling Program, College Station, TX, pp. 469–479.

Wetzel, A., 1991. Ecologic interpretation of deep-sea trace fossil communities. Palaeogeogr. Palaeoclimatol. Palaeoecol. 85 (1–2), 47–69.

Wetzel, A., 2008. Recent bioturbation in the deep South China Sea: a uniformitarian ichnologic approach. Palaios 23, 601–615.

Yin, Q.Z., Berger, A., 2012. Individual contribution of insolation and CO2 to the interglacial climates of the past 800,000 years. Clim. Dyn. 38, 709–724.

Young, J.R., Geisen, M., Cros, L., Kleijne, A., Sprengel, C., Probert, I., Østergaard, J., 2003. A guide to extant coccolithophore taxonomy. J. Nannoplankton Res. 1, 1–132. Special Issue.

Young, J.R., Bown, P.R., Lees, J.A. (Eds.), 2021. Nannotax3 Website. International Nannoplankton Association, 1 Sep. 2021. URL: http://ina.tmsoc.org/Nannotax3.